Angewandte Chemie

DOI: 10.1002/ange.201307851

Photocatalysis Hot Paper

Visible-Light Photocatalytic Conversion of Carbon Monoxide to Methane by Nickel(II) Oxide**

Francesc Sastre, Avelino Corma, and Hermenegildo García**

Research in the area of "solar fuels" obtained photocatalytically by sunlight is actual and active because these fuels are sustainable and CO_2-neutral. Although H_2 generation from H_2O is the most widely studied photocatalytic process for solar fuel production, the technical problems associated with H_2 storage and fuel-cell efficiency make also attractive other chemicals obtained from CO_2 such as CH_3OH, CH_4, and CO.[1–7]

The production of solar fuels requires efficient photocatalysts with high visible-light photoresponse. While TiO_2 is the most widely studied photocatalyst,[8–10] this semiconductor shows activity only upon UV-light exposure and a considerable effort aims at developing TiO_2 photocatalysts with visible response.[11–15] In contrast, the use of p-type semiconductors absorbing visible light such as NiO, CuO_x, FeO_x, and CoO_x has been less explored in photocatalysis, because of their presumably lower stability compared to TiO_2.[16] In particular, NiO has been frequently employed as co-catalyst in combination with titanates or other photocatalysts for visible-light splitting of H_2O rather than as active photocatalyst. In the present report, we describe that p-type semiconducting metal oxides, specifically NiO and FeO_x, show high visible and sunlight photocatalytic activity for the reduction of CO by H_2O vapor or H_2 leading to the formation of substantial amounts of CH_4, with almost complete selectivity at full CO conversion. NiO can be reused without change in the XRD pattern, supporting its photostability. The novelty of our study derives from the consideration of two points: 1) the unprecedented room-temperature photocatalytic CO reduction by H_2O or H_2 to CH_4, and 2) the possibility of using sunlight and visible light to activate the process.

Preliminary experiments using TiO_2 as photocatalyst showed that this n-type semiconductor leads mainly to oxidation of CO by H_2O vapor, forming quasi-stoichiometric amounts of CO_2 and H_2 [Eq. (1)],

$$CO + H_2O \xrightarrow[\text{photocatalyst}]{h\nu} CO_2 + H_2 (\Delta G^\circ = +31.36\ \text{kJ mol}^{-1}) \qquad (1)$$

accompanied by detectable, amounts of CH_4, and traces of ethane. Formation of CO_2 can be understood as arising from photooxidation of CO by positive holes generated in the charge separation on the semiconductor. The conversion of CO using TiO_2 promoted by solar light was very small (see Table 1) in agreement with the well-documented low photocatalytic activity of TiO_2 at solar light irradiation.[15]

Table 1: Photocatalytic activity for CO conversion, carbon content, and formation of H_2, CO_2 and CH_4 in the presence of metal-oxide semiconductors.[a]

Photocatalyst[b]	CO Conversion [%]	C [%][c]	Production [μmol g^{-1} cat.]		
			H_2	CO_2	CH_4[d]
TiO_2[e]	3	0.1	260	650	4 (0.5)
NiO[e]	95	3.3	820	12200	1700 (10.2)
CuO[e]	14	0.5	20	2900	270 (7.5)
Co_3O_4[e]	91	1.2	1000	12300	600 (4.3)
Co_2O_3[e]	93	3.1	990	12500	200 (1.3)
Fe_3O_4[e]	59	0.1	3620	8200	900 (9.8)
Fe_2O_3[e]	68	2.5	3760	10400	20 (0.2)
NiO[f]	96	2.2	–[g]	11240	8387 (39.1)
Fe_3O_4[f]	49	3.6	–[g]	6590	733 (7.1)
NiO[h]	99.5	1.8	–[g]	711	17266 (87)
Fe_3O_4[h]	28	0.5	–[g]	943	580 (28.2)
NiO[i]	99.4	1.9	–[g]	450	20799 (92)
NiO[j]	99.0	1.8	–[g]	87	16030 (97)
NiO[k]	16	1.0	–[g]	1386	1379 (38.3)

[a] Blank controls: 1) illumination in the absence of any solid, 2) contact to the solid and gas phase in the dark or 3) irradiation of the photocatalyst in N_2 did not lead to any product, C mass balances were higher than 95%. [b] See the Supporting Information for the origin and characterization data of these commercially available photocatalysts. [c] Weight percentage of carbon on the solid after the photocatalytic experiment. [d] The number in brackets corresponds to the selectivity of the process to CH_4 defined as number of moles formed of CH_4 divided by moles of converted CO in percentage. [e] Irradiation conditions: Mixture of N_2 (19.6 mmoles), H_2O (2.5 mmol), and CO (20%, 4.9 mmol), irradiation time 22 h, photocatalyst mass 250 mg, irradiation source solar simulator (1000 W m^{-2}). [f] Reaction conditions: Mixture of CO (20%, 5 mmol), H_2 (5 mmol), Ar (1.1 mmol), and N_2 (13.9 or 0.125 mmol); photocatalyst mass 250 mg, reaction time 3 h, light source solar simulator. [g] Reagent. [h] Reaction conditions: Mixture of CO (20%, 5 mmol), H_2 (18.75 mmol), Ar (1.1 mmol), and N_2 (13.9 or 0.125 mmol); photocatalyst mass 250 mg, reaction time 3 h, light source solar simulator. [i] Second test under conditions indicated in [h] and activation of NiO at 450 °C with air for 5 h. [j] Third test under conditions indicated in [h] and activation of NiO at 450 °C with air for 5 h.
[k] Irradiation with the solar simulator equipped with a cut-off filter ($\lambda > 400$) under conditions indicated in [h].

---

[*] Dr. F. Sastre, Prof. Dr. A. Corma, Prof. Dr. H. García
Instituto Universitario de Tecnología Química CSIC-UPV
Universidad Politécnica de Valencia
Avenida De los Naranjos s/n, 46022 Valencia (Spain)
E-mail: acorma@itq.upv.es
hgarcia@qim.upv.es

[**] Financial support by the Spanish Ministry of Economy and Competitiveness (MINECO) through several actions (Severo Ochoa and grant number CTQ 2012-32315) is gratefully acknowledged.

Supporting information for this article is available on the WWW under http://dx.doi.org/10.1002/anie.201307851.

Then we tested other first-row transition-metal oxides that can absorb visible light, though they are generally considered much less efficient photocatalysts than TiO_2. The results obtained for the p-type metal-oxide semiconductors are summarized in Table 1, whereas Figure S1 (see the Supporting Information) shows the temporal evolution of CH_4 upon irradiation in the presence of the p-type semiconductors using simulated solar light.

In contrast to experiments performed in the dark, where no products are formed (see footnote [a] in Table 1), or in contrast to the generation of CO_2 using TiO_2, p-type semiconducting metal oxides of Ni, Cu, Fe, and Co afford significant amounts of CH_4 in the gas phase upon sunlight irradiation. Equation (2) provides the presumed stoichiometry of the CH_4 formation for the photocatalytic CO reduction by water using simulated solar light.

$$CO + 2\,H_2O \rightarrow CH_4 + 1.5\,O_2 \;(\Delta G^0 = 541\ \text{kJ}\,\text{mol}^{-1}) \qquad (2)$$

While TiO_2 is a white powder, all the rest of the transition metals in Table 1 are colored, the visible absorption bands being responsible for the notable sunlight photoactivity (up to 33 times that of TiO_2). Particularly notable is the performance of NiO and Fe_3O_4 (in its most abundant α-polymorph)[17] where the production of CH_4 is the highest (10.2% in the gas-phase mixture in the case of NiO). These differences in photocatalytic activity in the series of p-type metal-oxide semiconductors are unlikely to arise from differences in their surface area, since they show similar values (see Table S1). It is more reasonable to attribute the results to the intrinsic photocatalytic properties (redox potentials of electrons and holes, efficiency of charge separation and lifetime of charge separation among other parameters to be considered) of the semiconductor.

Figure 1 shows the temporal evolution of the CO conversion and the formation of CO_2, CH_4, and H_2 using NiO as photocatalyst and H_2O as reducing agent under simulated sunlight irradiation. As can be seen in Figure 1, H_2 is formed as primary, but unstable product and its proportion grows in the first hour of irradiation, but subsequently decreases gradually. CH_4 exhibits an induction period at initial times and is formed as a secondary product. These temporal profiles, particularly the fact that the rate of H_2 decrease is about one half that of the CH_4 growth, provide kinetic support to a CH_4 formation mechanism involving prior generation of H_2 from H_2O vapor and subsequent reaction of H_2 to form CH_4.

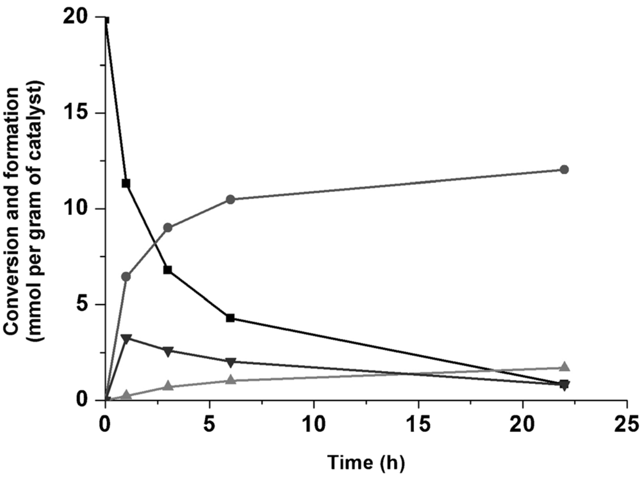

Figure 1. Photocatalytic CO (■) conversion and formation of CO_2 (●), CH_4 (▲) and H_2 (▼). Reaction conditions: gas-phase irradiation of a moisture-saturated mixture of N_2 (80%) and CO (20%, 4.9 mmol), NiO 250 mg, irradiation source solar simulator (1000 W × m^{-2}).

With regard to Table 1, it is worth commenting on the high percentage of carbon present on the solid photocatalyst, particularly in the cases of NiO, Co_2O_3, and Fe_2O_3. This carbonaceous residue adsorbed on the photocatalyst was characterized by Raman and X-ray photoelectron spectroscopy (XPS; see Figures S2 and S3), both spectra being compatible with the assignment of this residue to graphitic carbon generated in the photocatalytic process. The fresh photocatalysts do not show any carbon-related Raman peak. However, after irradiation, the characteristic 2D, G, and D bands of carbon appearing between 2500–2900 and at 1600 and 1350 cm^{-1} were observed.

XPS of the photocatalyst after being used shows the presence of a peak at 285.12 eV that can be deconvoluted in three major components corresponding to sp^2 graphene C atoms (67%), sp^2 C atoms bonded to O (25%), and sp^3 C atoms (8%), respectively. The percentage of carbonaceous residue deposited on each material before and after irradiation was determined by combustion elemental analysis of the solid. The carbon content of the fresh photocatalysts was negligible, whereas it was necessary to consider the amount of carbon deposited on the photocatalyst after the reaction, together with the CH_4 and CO_2 formed in the gas phase to calculate satisfactorily the C mass balance (> 95%) in all cases. This indicates that CO is converted not only into gas-phase products, but it also forms carbon deposits on the solid. In agreement with the presence of carbon on the used photocatalyst, the colored metal oxides after the reaction become in some cases visually black (see the inset in Figure S2 for NiO).

The behavior observed for p-type semiconductors (formation of large CH_4 percentages in the gas phase and carbon residues on the solid) sharply contrasts with the photocatalytic activity of TiO_2 commented earlier [Eq. (1)]. Additional tests using CeO_2 as photocatalyst, another n-type semiconductor, also show the preferential formation of CO_2. Sunlight conversion of CO using TiO_2 and CeO_2 is about 30 times lower than the conversion achieved by p-type metal oxides. This low activity of TiO_2 and CeO_2 at solar light irradiation is well-known and derives from their limited visible-light photoresponse of these wide-bandgap semiconductors. Besides the advantageous photoaction spectra of n-type semiconductors arising from the visible-light absorption of these materials, the different photocatalytic behavior of p- and n-type semiconductors could derive from the higher conduction-band potential in p-type semiconductors (+ 0.8 V versus the normal hydrogen electrode, NHE, for Ni)[18] compared to TiO_2 (−0.1 V versus NHE at pH 0)[19] and CeO_2 (−0.1 V).[12] A high conduction band potential favors the reduction of CO to C and CH_4 with respect to the oxidation of CO to CO_2 which is almost the sole process observed for TiO_2 and CeO_2.

To establish if the photocatalytic reduction of CO to CH_4 using p-type photocatalyst can be further favored using H_2 instead of H_2O as reducing agent present in the system, additional experiments with simulated sunlight where NiO or Fe_3O_4 were illuminated in contact with an atmosphere that contains CO and H_2 were carried out. H_2 could be obtained independently from steam reforming and the water-gas shift reaction or generated photocatalytically from water. The results obtained using two different CO/H_2 molar ratios are summarized in Table 1 (footnotes [f] and [h]), whereas the corresponding time conversion plots are shown in Figure 2.

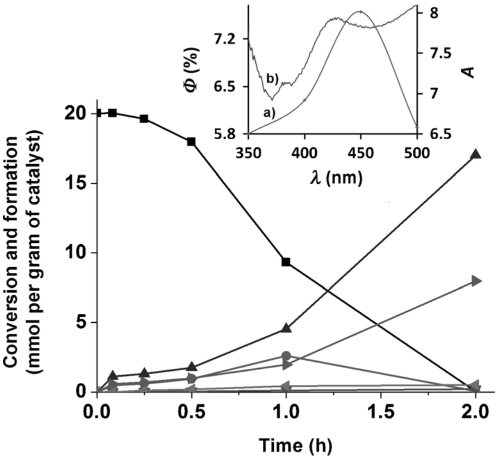

Figure 2. CO (■) conversion and formation of CO_2 (●) and CH_4 (▲), O_2 (▶), ethane (◀) and propane (▼). Reaction conditions: Mixture of CO (20%, 5 mmol), H_2 (18.75 mmol), Ar (1.1 mmol), and N_2 (13.9 or 0.125 mmol); photocatalyst mass 250 mg, reaction time 3 h, light source solar simulator, illumination source solar simulator (1000 W×m^{-2}). The inset shows the apparent quantum yields (*Φ*) for the CH_4 formation (a) and the UV/Vis absorption spectrum of NiO (b; *A* = absorbance).

The photocatalytic CH_4 formation increases considerably using H_2 as reducing agent. The high CO conversions achieved using H_2 allow the quantification of the O_2 evolution, which shows a trend similar to the temporal profile of the CH_4 evolution (Figure 2) according Equation (3).

$$CO + 2\,H_2 \rightarrow CH_4 + 0.5\,O_2 (\Delta G^0 = +35.6\ \mathrm{kJ\,mol^{-1}}) \quad (3)$$

Both in the absence and presence of H_2, formation of CO_2 is observed although with considerably lower yields when H_2 is present (see Table 1 and Figure 2). This higher activity using H_2 as reducing agent can be easily understood considering the high endoergonicity of the reaction using H_2O as reducing agent [Eq. (2)] and the more complex reaction mechanism using H_2O that requires prior H_2 generation. The percentage of elemental carbon deposited on NiO is reduced by one half when the irradiation is carried out using H_2 as reducing agent compared to H_2O vapor.

For the formation of CH_4 two equivalents of H_2 should be consumed. Thus, for those irradiation reactions where H_2 and CO are present in a 1:1 molar ratio, the generation of CH_4 reaches asymptotically a value that does not grow further when the reaction time is prolonged (Figure S4). When the irradiation is carried out in H_2 excess, the CH_4 production is higher, the consumption of CO is complete, and the percentage of CO_2 formed is considerably lower.

Comparison of the photocatalytic activity of NiO and Fe_3O_4 indicates that the former is more efficient for the CH_4 formation (Table 1). The highest CH_4 yield achieved herein was 17.26 mmol per gram of catalyst, corresponding to a reaction carried out using NiO as photocatalyst with a 3.5-fold excess of H_2. Under these optimal conditions in excess of H_2 using simulated sunlight with a nominal power of 1000 W×m^{-2}, the yield of CO_2 is 24 times lower than the global amount of alkanes. This efficiency using simulated solar light is remarkable and without precedent.

To assess the visible-light photoactivity of NiO, the photoaction spectrum for the CH_4 generation was determined (see the inset in Figure 2). The overlay of the apparent quantum yield for the CH_4 generation based on the incident photon conversion (maximum Φ_{app} 7.5% at 450 nm) with the NiO absorption band shows a notable coincidence, although the efficiency of the photocatalytic CH_4 generation at long wavelengths is much lower compared to the NiO absorption spectrum. This could be related to the higher efficiency of the ligand-to-metal electronic transition appearing around 410 nm with respect to the less efficient Ni^{2+}-centered d–d absorption characteristic of transition-metal ions with incomplete d shell appearing at longer wavelengths in the visible region.

In cases in which H_2 is present together with CH_4, significant amounts of ethane and propane are also formed. Formation of these light alkanes decreases somewhat the CH_4 selectivity. This behavior is reminiscent of the Fischer–Tropsch process, where a mixture of CO and H_2 gives rise to the formation of linear hydrocarbon molecules at elevated temperatures using Ni or Fe catalysts. It is, however, pertinent to remind that the current process is performed at temperatures below 36 °C.

Formation of elemental carbon on the photocatalyst corresponds to CO reduction and this elemental carbon could act as an intermediate in the formation of CH_4. In order to verify this possibility, a test was carried out in which CO diluted in N_2 was submitted to irradiation until the NiO photocatalyst became visually black. At this time, the irradiation was stopped and the photoreactor outgassed to remove CO. Sampling of the photocatalyst revealed 1.7 wt% carbon content. Then, H_2 was admitted into the photoreactor and the irradiation continued. CH_4 evolution was observed in the gas phase in the absence of CO. This experiment can be easily interpreted considering that upon irradiation in the absence of H_2 carbon deposits are formed on the NiO surface. Subsequently, this carbon residue is able to react photocatalytically with H_2 to form CH_4, regardless of the absence of CO. A control experiment following an identical protocol in the dark shows that no CH_4 is formed.

A mechanistic proposal for the photoreduction of CO by H_2 using a p-type photocatalyst is shown in Scheme 1. According to this proposal, CO can act as a hole-trapping

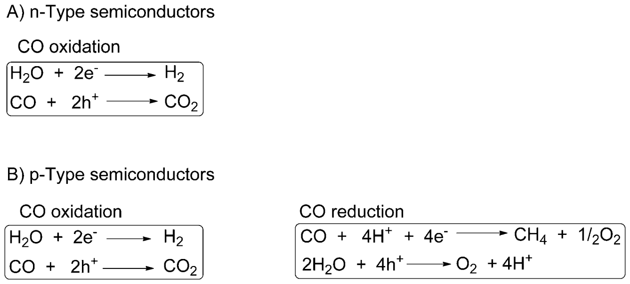

Scheme 1. Contrasting photocatalytic behavior of n- and p-type semiconductors based on the product distribution observed.

agent, leading to the formation of CO_2. If another electron donor agent, such as H_2O or H_2, is also present, then these compounds will compete with CO for oxidation. CO can alternatively undergo reduction by the semiconductor conduction-band electrons, forming elemental C and O_2. This CO reduction process will be more favorable as the reduction potential of the conduction-band edge of the photocatalyst increases (case of p-type semiconductors), as has been observed in related precedents.[20] Thus, one of the main factors influencing the outcome of the photocatalytic CO reduction should be the position of the semiconductor conduction-band edge.

In agreement with this rationalization, a stoichiometric growth in the concentration of molecular O_2 was detected when H_2 is the reducing agent. When H_2O is used as electron donor, the lower formation of CH_4 makes the quantification of O_2 uncertain because of the air contamination. Elemental carbon is deposited on the surface of the photocatalyst as evidenced visually (inset in Figure S2) and determined by combustion chemical analysis (Table 1). Elemental carbon undergoes efficient photocatalytic H_2 reduction, giving rise to CH_4.

To provide some support to the mechanistic proposal, additional experiments were carried out. A mixture of CO and H_2 was irradiated in the presence of methanol as sacrificial electron donor agent, whereby total inhibition of the formation of CO_2 was observed, while CH_4 was still formed. This is in accordance with the proposed origin of CO_2 arising from the photooxidation of CO on the surface of the semiconductor as indicated in Scheme 1.

The photocatalytic irradiation of CO and H_2 using simulated sunlight was also performed in the presence of CH_4 and NiO as photocatalyst, and under these conditions ethane as primary irradiation product was observed, similar to the Fischer–Tropsch mechanisms and the reported photocatalytic CH_4 conversion.[21]

One of the main reasons frequently invoked to disregard p-type semiconducting metal oxides as photocatalysts is their presumed lack of stability and the occurrence of corrosion. Photocorrosion tests have been carried out mainly in liquid water. Since these conditions are different from those employed in the present study in the gas phase, we have verified the stability of the photocatalytic activity of NiO by performing three consecutive tests of the same sample. After each test, the NiO sample was submitted to calcination at 450 °C in air to effect the combustion of possible carbonaceous residue. As can be seen in Table 1, a minor decay in the CO conversion (from 99.5 to 99 %) and even an increasing CH_4 selectivity (from 87 to 97 %) were measured after the three tests. Moreover, XRD of the NiO sample before and after the three tests was also coincident, ruling out changes in the crystal structure of NiO. XPS, which is a specific surface analysis technique, did not show differences in the binding energy related to the Ni 2p peaks (Figure S5). This information indicates the stability of NiO as photocatalyst under the present conditions. A similar stability was observed by XPS for Fe_3O_4 and Co_3O_4 (Figures S6–S8)

The previous photocatalytic experiments were carried out using simulated sunlight containing about 5 % UV radiation. The high photocatalytic activity in terms of CO conversion using NiO as catalyst compared to TiO_2 or CeO_2 has been attributed to the visible-light photoresponse of NiO in accordance to the photoaction spectrum. Additional experiments on the photocatalytic reduction of CO to CH_4 by H_2 using NiO were also carried out under visible-light irradiation using a filter that cuts off radiation wavelengths shorter than 400 nm (see the spectrum of the cut-off filter in Figure S9). The results of the visible-light photocatalytic activity of NiO (see Table 1) show that although a large percentage of the catalytic activity of NiO is related to the UV region, NiO is still active under visible-light illumination.

In conclusion, here we have shown that p-type transition-metal oxide semiconductors are efficient photocatalysts for the visible-light or solar-light, room-temperature reduction of CO to CH_4, provided that H_2O vapor or H_2 are present as reducing agents. This photochemical behavior contrasts with that of TiO_2 and CeO_2 (n-type semiconductors) that promote under the same conditions highly selectively the oxidation of CO to CO_2. Formation of elemental carbon deposited on the photocatalyst surface is also observed. NiO was the most efficient photocatalyst among the series of first-raw transition-metal oxide semiconductors. Under optimal conditions using simulated sunlight and molecular H_2 as reducing agent, a selectivity towards the formation of CH_4 of 97 % at complete CO conversion was obtained. Our results open new opportunities for the photocatalytic production of solar fuels at high conversion and selectivity.

Received: September 6, 2013

Keywords: methane formation · metal oxides · photocatalysis · semiconductors · solar fuels

---

[1] G. R. Dey, *J. Nat. Gas Chem.* **2007**, *16*, 217.
[2] S. Navalón, A. Dhakshinamoorthy, M. Álvaro, H. Garcia, *ChemSusChem* **2013**, *6*, 562.
[3] J.-S. Hwanga, J.-S. Changa, S.-E. Parkb, K. Ikeuec, M. Anpo, *Top. Catal.* **2005**, *35*, 311.
[4] T. Inoue, A. Fujishima, S. Konishi, K. Honda, *Nature* **1979**, *277*, 637.
[5] K. Koci, L. Obalová, L. Matejová, D. Plachá, Z. Lacný, J. Jirkovský, O. Solcová, *Appl. Catal. B* **2009**, *89*, 494.
[6] W. Leitner, *Angew. Chem.* **1995**, *107*, 2391; *Angew. Chem. Int. Ed. Engl.* **1995**, *34*, 2207.

[7] K. Mori, H. Yamashita, M. Anpo, *RSC Adv.* **2012**, DOI: 10.1039/c2ra01332k.
[8] M. A. Fox, M. T. Dulay, *Chem. Rev.* **1993**, *93*, 341.
[9] M. R. Hoffmann, S. T. Martin, W. Y. Choi, D. W. Bahnemann, *Chem. Rev.* **1995**, *95*, 69.
[10] D. W. Bahnemann, *Res. Chem. Intermed.* **2000**, *26*, 207.
[11] A. Primo, A. Corma, H. Garcia, *Phys. Chem. Chem. Phys.* **2011**, *13*, 886.
[12] A. Primo, T. Marino, A. Corma, R. Molinari, H. Garcia, *J. Am. Chem. Soc.* **2011**, *133*, 6930.
[13] S. Sakthivel, M. Janczarek, H. Kisch, *J. Phys. Chem. B* **2004**, *108*, 19384.
[14] S. Sakthivel, M. V. Shankar, M. Palanichamy, B. Arabindoo, D. W. Bahnemann, V. Murugesan, *Water Res.* **2004**, *38*, 3001.
[15] C. G. Silva, R. Juarez, T. Marino, R. Molinari, H. Garcia, *J. Am. Chem. Soc.* **2011**, *133*, 595.
[16] J. M. Herrmann, *ACS Symp. Ser.* **1986**, *298*, 200.
[17] G. Carraro, C. Maccato, A. Gasparotto, T. Montini, S. Turner, O. I. Lebedev, V. Gombac, G. Adami, G. Van Tendeloo, D. Barreca, P. Fornasiero, *Adv. Funct. Mater.* **2013**, n/a.
[18] M. P. Dare-Edwards, J. B. Goodenough, A. Hamnett, N. D. Nicholson, *J. Chem. Soc. Faraday Trans. 2* **1981**, *77*, 643.
[19] M. Grätzel, *Nature* **2001**, *414*, 338.
[20] Y. P. Xie, G. Liu, L. Yin, H.-M. Cheng, *J. Mater. Chem.* **2012**, *22*, 6746.
[21] L. Yuliati, H. Yoshida, *Chem. Soc. Rev.* **2008**, *37*, 1592.